ACS ES&T Water

Open Access

pubs.acs.org/estwater

Article

Influence of Multiple Parameters on Groundwater Iron Removal in the Presence of Ammonium Nitrogen

Valentin Romanovski,* Elena Velyugo, and Viktor Yushchenko

Cite This: ACS EST Water 2026, 6, 1083−1097

Read Online

ACCESS | Metrics & More | Article Recommendations | Supporting Information

ABSTRACT: This paper studies the effect of the initial iron (2.1−6.9 mg/L) and ammonium nitrogen (2.5−6.0 mg/L) concentrations and aeration parameters on the efficiency of two-stage purification of complex groundwater. The experimental setup utilized two stages of filters with air-to-water ratios of up to 5:1 and 1.5:1, respectively. It was found that secondary aeration reduced residual iron to the standard 0.3 mg/L, while the ammonium nitrogen concentration dropped below 1.5 mg/L in most modes. The maximum efficiency of ammonium removal was observed with optimal second-stage aeration: in the absence of aeration, the purification efficiency was only 39.5%, while with optimal parameters, the efficiency reached 75−80%. Correlation analysis revealed the key role of the initial concentrations and aeration parameters: for iron, the critical factor was Fe^{2+} and its interaction with N-NH_4^+, and for ammonium nitrogen, it was the intensity of second-stage aeration. Machine learning models (CatBoost and GPR) showed R^2 determination coefficients of up to 1.000, confirming the high accuracy of forecasting. Practical implementation of the second stage of purification at the station made it possible to reduce residual iron concentrations by an additional 35−45% and reduce energy costs by 15−20% due to aeration optimization, ensuring stable compliance with Fe and N-NH_4^+ standards.

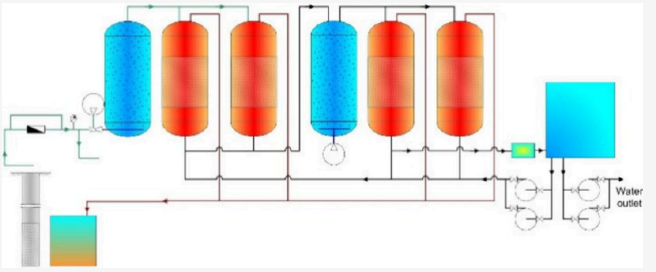

KEYWORDS: *groundwater, iron removal, ammonia nitrogen, aeration, machine learning*

1. INTRODUCTION

Natural underground aquifers often contain elevated levels of iron and ammonium nitrogen, which create serious environmental and sanitary problems.[1] High concentrations of iron and associated manganese in water lead to deterioration of its organoleptic characteristics, sediment formation, and corrosion of pipelines and can also have a negative impact on human health with long-term consumption. Similarly, excess organic and ammonium substances in water pose a health hazard to the population, causing metabolic disorders and increasing the risk of developing cancer.[2,3] Water containing iron, manganese, organic matter, and ammonium has a complex composition that complicates its treatment. The relevance of the topic is due to the need to develop effective technologies for removing these pollutants from natural water, considering the characteristics of small settlements, where traditional purification methods are often insufficiently effective or economically infeasible.[4,5] Treatment processes are complicated by differences in the chemical properties and oxidation−reduction potential of the pollutants present, which require the use of integrated treatment approaches.

Today, there are a wide range of methods for removing iron from groundwater. Traditional technologies include aeration with subsequent filtration through granular media,[4−7] the use of modified anthracites,[8,9] and activated carbons,[10] as well as biological[11,12] and integrated methods.[13] These approaches can effectively reduce the concentration of dissolved iron to standard values, provided that the operating conditions are correctly configured.

The removal of ammonium nitrogen is a more complex task. Traditional methods include the use of minerals,[14] activated carbons,[15] and biological treatment—nitrification followed by a denitrification stage.[16] In recent years, special attention has been paid to membrane technologies: ultrafiltration,[17] nanofiltration, and membrane bioreactors,[18,19] which allow one to achieve high degrees of purification provided that the water is pretreated but also significantly increase the cost of the purification system. Nanomaterials based on metal dioxides,[20,21] which have high selectivity to pollutants, are also being actively developed.

However, in the presence of ammonium nitrogen, the efficiency of groundwater purification from iron is significantly reduced.[22] There is a need to use complex technologies for groundwater treatment with the simultaneous removal of all impurities as well as the selection of the sequence of substance

Received: September 25, 2025
Revised: January 14, 2026
Accepted: January 14, 2026
Published: January 26, 2026

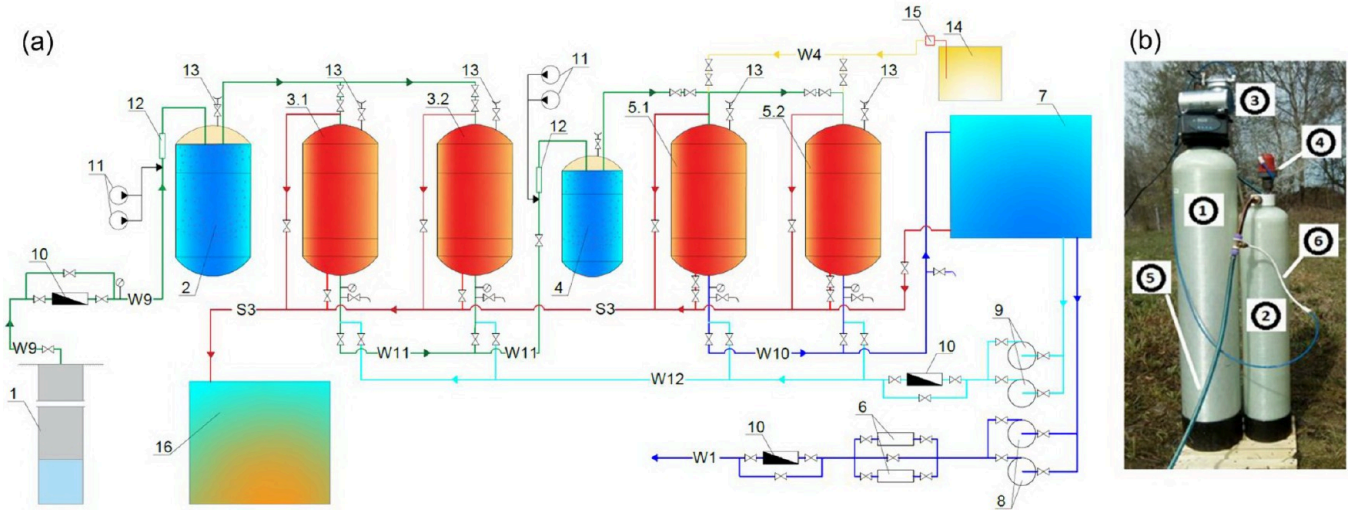

Figure 1. (a) Flowchart of groundwater purification: 1, well; 2, first-stage aeration column; 3, first-stage filters (AC sorbent loading); 4, second-stage aeration column; 5, second-stage filters (zeolite loading); 6, water disinfection; 7, clean water tank; 8, second lift pumps supplying water to the consumer; 9, pumps supplying wash water to the filters; 10, water meters for the original, purified, and wash water; 11, compressor; 12, mixer; 13, plunger; 14, salt dissolver tank; 15, dosing pump; 16, wash water settling tank; W9, pipeline supplying original water to the filters; W11, water discharge after the first-stage filters; W1, pipeline supplying purified water to consumers; W4, pipeline for feeding table salt solution to regenerate second-stage filters; W10, discharge of purified water after iron removal filters to the clean water tank; W12, pipeline for feeding wash water from the clean water tank; S3, pipeline for discharge of spent wash water to settling tanks. (b) Experimental setup for conducting an experiment with an aeration column: 1, main column with loading, 250 mm in diameter; 2, aeration column; 3, compressor; 4, siphon; 5, feedwater supply; 6, air supply.

treatment, considering their oxidation–reduction properties. Of particular importance is the integration of oxidation methods with subsequent sorption for the complex purification of water of complex composition. Also, because the task of the water supply and sewerage system is to use available materials and reliable technologies, the most frequently used main component in the oxidation of groundwater is atmospheric oxygen. However, as the practice of operating pressure filters of iron removal stations for small settlements shows, the level of its content in most cases is insufficient even to meet the standardized requirements for the removal of total iron. Therefore, in addition to the aeration of water with atmospheric oxygen, an important aspect is the selection of optimal materials for loading filters and process conditions, which allows for increasing the efficiency of contaminant removal at minimal cost. Conducting comprehensive studies to optimize existing process flowcharts[23,24] will improve water quality while reducing costs and expanding the possibilities for upgrading existing facilities.

For a comprehensive analysis of the efficiency of groundwater purification technologies for iron in the presence of ammonium nitrogen, it is necessary to consider a wide range of parameters, including the initial concentrations of pollutants, oxidation–reduction potential, pH, dissolved oxygen (DO) content, and aeration modes, as well as some organizational issues.[25] Of particular relevance is the use of mathematical modeling, including modern machine-learning algorithms that allow one the identify hidden relationships between the process factors and purification quality. Such models provide the ability to promptly select optimal aeration and filtration conditions depending on the water composition and regulatory requirements, which significantly increases the adaptability and energy efficiency of water treatment systems.

Despite extensive research on iron and ammonium removal, the simultaneous presence of Fe^{2+} and N-NH_4^+ creates a complex treatment environment. This environment is governed by strongly nonlinear and oxygen-dependent interactions. These interactions are not adequately described by traditional empirical or single-factor models. Multistage filtration systems further increase the dimensionality of the problem because the aeration intensity, redox conditions, iron oxidation kinetics, sorption behavior, and biofilm activity act concurrently. In this context, machine-learning regression methods provide a distinct advantage: they allow the extraction of multidimensional patterns from limited but well-structured experimental data sets, quantify the relative importance and competition of key factors, and generate compact predictive equations for operational optimization. By integrating ML-based regression with controlled laboratory experiments, this study introduces an innovative framework for analyzing Fe/N-NH_4^+ coexistence in groundwater treatment and for identifying aeration regimes that maximize purification efficiency.

The objectives of the work were as follows: (i) experimentally study the effect of the initial concentrations of total iron and ammonium nitrogen, as well as the aeration parameters at the first and second stages, on the efficiency of two-stage purification of groundwater of complex composition; (ii) build and compare mathematical models (regression, polynomial, and machine-learning methods) for the quantitative description and prediction of residual concentrations of iron and ammonium nitrogen in purified water; (iii) determine key control factors and establish optimal air–water ratios at both stages of purification, ensuring compliance with regulatory indicators for iron and ammonium nitrogen; (iv) compare the modeling results with experimental data to verify the models and assess their practical applicability in real water treatment facilities.

In contrast to our previous studies,[23,24] which investigated isolated aspects of groundwater purification, the present research provides a fundamentally broader analysis. Work[23]

https://doi.org/10.1021/acsestwater.5c01127
ACS EST Water 2026, 6, 1083–1097

examined only the qualitative influence of ammonium nitrogen on the efficiency of iron removal within a single-stage filtration system, without assessing the operational aeration parameters or quantitative interactions between Fe^{2+} and N-NH_4^+. The study[24] focused primarily on the design of a new granulated filter for joint Fe/N-NH_4^+ removal and did not evaluate multistage treatment, aeration regimes, or process modeling.

The scientific novelty of this work is determined by four key elements: (i) experimental investigation of a two-stage purification scheme with an independently adjustable aeration intensity at each stage; (ii) implementation of a multifactor experiment (29 modes) covering wide ranges of Fe, N-NH_4^+, and aeration values; (iii) quantitative correlation and kinetic analysis, revealing the mechanistic interaction between ammonium nitrogen and iron oxidation; (iv) development of predictive machine-learning models (CatBoost, GPR, and ElasticNet-poly) that allow real-time determination of the optimal aeration settings and reach coefficients of determination of up to R^2 = 1.000. None of these aspects were addressed in ref 23 or ref 24, which demonstrates the substantial advancement introduced in the present study.

2. MATERIALS AND METHODS

2.1. Characteristics of Groundwater

The object of the study was groundwater with a complex water composition in the western part of the Vitebsk region (Belarus). According to the monitoring results in this area, a complex composition of groundwater is observed in about 60% of water supply sources. In this case, not only iron but also manganese, ammonia in the form of ammonium nitrogen, and permanganate-based chemical oxygen demand (COD-Mn) are contained above the standard values, which can affect the choice of water treatment technology. For the experiment, a small water supply object in the Vitebsk region was selected, the groundwater of which at different times contained an iron concentration of 2.1−6.9 mg/L, ammonium nitrogen N-NH_4^+ of 2.5−6.0 g/L, a pH between 7.3 and 7.5, and COD-Mn of 4.2−8.0 mgO_2/L. The depth of the water intake wells was 60−80 m. The existing standard purification scheme, including an aeration column and a pair of filters (one purification stage), did not ensure the purification of water for iron and ammonium nitrogen to standard values.

2.2. Description of the Process Flow Scheme

The conducted research results for processing complex composition of underground water[23] showed high efficiency of using a two-stage filtration scheme using AC sorbents[26] at the first stage and Zeol brand zeolite[27,28] at the second stage. Before each filter stage, the process layout included intensive aeration using an aeration column and a compressor (Figure 1a). It should be noted that the first stage of purification is the existing official version of the water treatment plant and the second stage is experimental.

The experiment was conducted at the existing iron removal station (the first stage of purification), which operated according to a parallel process scheme with an aeration column and two pressure filters with a diameter of 0.5 m each, a filtration area of 0.2 m^2, and a filtration rate of 6.25 m^3/h. The filter load with a height of 1 m was represented by the AC sorbent with a fraction diameter of 0.7−1.2 mm. The station capacity was 2.5 m^3/h. The filters were backwashed by pumps from a tank with a capacity of 5 m^3. The pilot unit (the second stage of purification) was connected to the pipeline after the water iron removal filters (Figure 1b). The pilot unit consisted of an aeration column and a filter with a diameter of 0.25 m with a load of Zeol zeolite with a volume of 25 L. The filtration rate was 10 m/h, and the flow rate was 0.49 m^3/h. Before the experiments, the filter load in the pilot plant was regenerated with an 8% sodium chloride solution.

The air−water ratio in the aeration column before the first-stage filters varied to 5:1 and that before the second-stage filters to 1.5:1. The filtration unit operated continuously for 3 h in each mode to stabilize the residual concentrations of ammonium and iron. After this, samples were taken. Water samples were taken at three points: the initial point and after the first- and second-stage filters. In the proposed water purification scheme, the measured parameters were as follows: iron concentration C_{Fe} (mg/L), ammonium nitrogen $C_{NH_4^+}$ (mg/L), COD-Mn (mgO_2/L), pH, Eh, and DO values in the initial water and at the outlet after the first and second stages; the degree of air volume saturation per unit volume of water (before the first stage of filters), A1 (m^3/m^3); the degree of air volume saturation per unit volume of water (before the second stage of filters), A2 (m^3/m^3). The particle size of the filter media was not varied in this study. The granular materials employed in both stages correspond to the standard particle-size ranges commonly used in groundwater iron-removal and ammonium-removal filters, as recommended in practical design guidelines. Because the objective of the present work was to analyze Fe/NH_4^+ interactions and aeration-dependent behavior under typical operational conditions, variation of the media grain size was not considered as an independent experimental factor.

2.3. Determination of the Water Composition

To conduct experimental studies, we used devices that had verification certificates for the period of the studies: a drying cabinet, laboratory scales, magnetic stirrers, and EM-NO3-07 and EVL-1M3.1 membrane electrodes. The indicators were determined after 10 h of filter operation after the operating efficiency was reached.

Determination of the concentration of total iron in purified groundwater in pilot experiments was based on the interaction of iron ions in an alkaline medium with sulfosalicylic acid to form a yellow complex compound. The pH of the original and purified water was measured according to ISO 10523-2009. Ammonium ions were determined according to GOST 33045-2014 method A, and DO was determined using a portable waterproof oxygen meter HI9146-04. The COD-Mn determination was carried out by heating the test sample in a boiling water bath with a known amount of potassium permanganate solution and sulfuric acid for a certain period of time (10 min). Some of the permanganate ions were reduced by oxidizable substances contained in the sample, and their remains reacted with a sodium oxalate solution added in excess. Excess sodium oxalate was titrated with potassium permanganate solution STB ISO 8467-2009. Three samples were analyzed in parallel for each parameter.

2.4. Mathematical Analysis

As part of the processing of the obtained experimental data, a comprehensive mathematical analysis was carried out to assess the correlation and interrelations between the parameters and their impact on the final concentration of iron and ammonium nitrogen, including the construction of the Pearson matrix and the subsequent selection of the optimal model for regression analysis and machine learning. The construction, training, and validation of models [polynomial regression, elasticnet, elasticnet with polynomial features, Lasso, CatBoost, eXGBoost, and Gaussian Process Regression (GPR)] were performed in the Python environment using the scikit-learn, CatBoost, XGBoost, SVR and Numpy/Pandas libraries. For each model, hyperparameters were optimized, the accuracy was assessed by the determination coefficient, and the significance of factors was analyzed. The following notations were used to analyze the correlation between factors: X1, concentration $Fe_{tot\ initial}$ (Fe_0), mg/L; X2, concentration ($N\text{-}NH_4^+{}_{initial}$), mg/L; X3, potential ($Eh_{initial}$), mV; X4, $pH_{initial}$; X5, concentration ($O_{2,initial}$), mg/L; X6, COD-$Mn_{initial}$, mgO_2/L; X7, V_1 (aeration on the first stage), m^3/m^3; X8, V_2 (aeration on the second stage), m^3/m^3; Y1, concentration (Fe_{tot} after the first stage), mg/L; Y2, concentration (N-NH_4^+ after the first stage), mg/L; Y3, potential (Eh after the first stage), mV; Y4, pH after the first stage; Y5, concentration (O_2 after the first stage), mg/L; Y6, COD-Mn after the first stage, mgO_2/L; Y7, potential (Eh after the second stage), mV; Y8, pH after the second stage; Y9, concentration (O_2 after the second stage), mg/L; Y10, COD-Mn after the second stage, mgO_2/L; Y11, concentration (Fe_{tot} after the second stage), mg/L; Y12, concentration (N-NH_4^+ after the second stage),

https://doi.org/10.1021/acsestwater.5c01127
ACS EST Water 2026, 6, 1083−1097

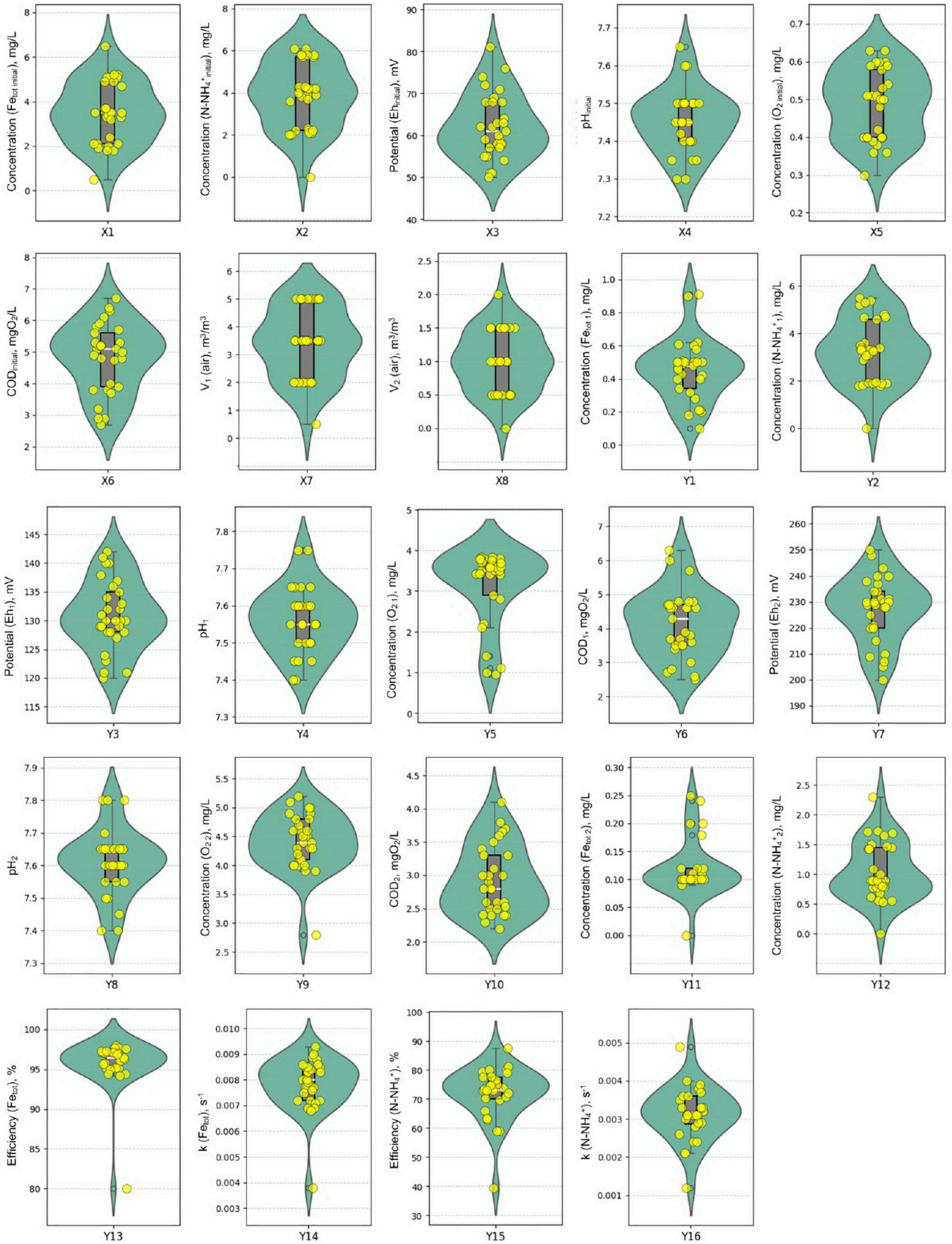

Figure 2. Variation ranges of parameters in the experiment (concentrations of Fe, $N\text{-}NH_4^+$, Eh, pH, O_2, COD, and aeration intensity) at the purification stages.

https://doi.org/10.1021/acsestwater.5c01127
ACS EST Water 2026, 6, 1083−1097

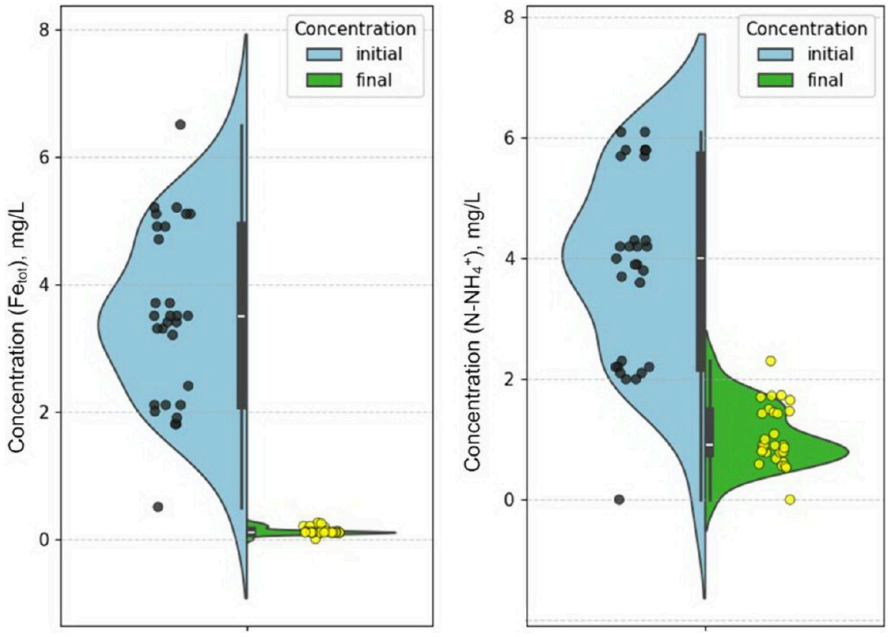

Figure 3. Total purification efficiency for Fe and N-NH_4^+ (comparison of the initial and output concentrations).

mg/L; Y13, efficiency (Fe_{tot}), %; Y14, k (Fe_{tot}), s^{-1}; Y15, efficiency (N-NH_4^+), %; Y16, k (N-NH_4^+), s^{-1}. The data set includes 29 experiments (SI_Data set.xlsx).

It should be noted that, in this work, the machine-learning algorithms (CatBoost, GPR, ElasticNet, and SVR) were used primarily as regression equation generators, aimed at obtaining compact nonlinear dependencies rather than developing predictive models in the classical sense. Given the limited data set (n = 29) and the physicochemical purpose of the analysis, the models were trained on the entire data set without train/test splitting, and cross-validation was not applied. This approach ensured the stability of the regression coefficients and preserved the interpretability required for technological optimization.

3. RESULTS AND DISCUSSION

3.1. General Analysis of the Installation Operation and Obtained Data Set

According to the obtained data (SI-file.xlsx), the use of the proposed water treatment scheme, including two aeration stages, made it possible to achieve the standard values for ammonium nitrogen. It was found that secondary aeration intensifies the processes of reducing iron concentrations and also significantly helps to reduce the content of ammonium nitrogen. In this regard, it was of interest to search for patterns in water purification from iron and ammonium nitrogen depending on their initial concentration, aeration intensity, and a number of other water parameters, with the aim of promptly optimizing the aeration intensity at each purification stage and providing standard values of purified water for total iron and ammonium nitrogen. For a comprehensive assessment of the performance of the developed two-stage purification scheme and to identify the influence of key operational parameters, a multifactorial experiment was planned and conducted. The ranges of variation of each of the measured parameters within the framework of the experiment are shown in Figure 2.

During the study, the upper level for iron was 5 mg/L, which significantly exceeds the maximum permissible concentration (MPC) for drinking water established by both the national standards of the Republic of Belarus (0.3 mg/L)[29] and the recommendations of the World Health Organization (WHO) (0.3 mg/L).[30] Similarly, the upper level for ammonium nitrogen (6 mg N/L) was significantly higher than the corresponding MPCs (1.5 mg N/L in Belarus[29] and 1.5 mg N/L as the WHO guideline value[30]). The study of such elevated concentrations allows us to estimate the maximum capabilities of the water treatment plant corresponding to severe cases of groundwater pollution and to ensure that standard values are achieved at typical pollutant concentrations. Varying the aeration intensity at the first stage aims to optimize the processes of Fe^{2+} oxidation to Fe^{3+} and subsequent hydrolytic precipitation of iron, as well as oxidation of the readily available organic fraction (COD-Mn) before the second stage. The ratio of air and water supply at the second stage allows determination of the need and optimal intensity of additional aeration immediately before the zeolite filter to maintain a high level of DO, which is critical for the catalytic oxidation of ammonium nitrogen and organic substances on the zeolite surface and the formation of a FeOOH layer. The overall assessment of the purification efficiency of the entire plant for the concentration of total iron (Fe) and ammonium nitrogen (N-NH_4^+) is shown in Figure 3.

The data analysis in Figure 4 clearly demonstrates the high efficiency of the proposed scheme for total iron and, in some cases, excess ammonium nitrogen. The final iron concentration consistently corresponds to the established MPC of 0.3 mg/L,[29,30] which confirms the reliable operation of the proposed scheme. This figure shows that the main challenge in purification is ammonium nitrogen, and the available range of concentrations at the inlet and outlet of the plant with the selected series of aeration efficiency will allow one to find the optimal conditions for the aeration intensity that provide the standard values. The concentration of N-NH_4^+ in the source water varied from 2 to 6.4 mg/L. After treatment at the plant, a decrease below 2.0 mg/L is observed. In most operating modes, especially with optimal aeration parameters at the second stage (X4), the final ammonium concentration consistently reaches values below the MAC of 1.5 mgN/L.[30] Thus, higher residual concentrations (1.5−2.0 mg/L) observed

https://doi.org/10.1021/acsestwater.5c01127
ACS EST Water 2026, 6, 1083−1097

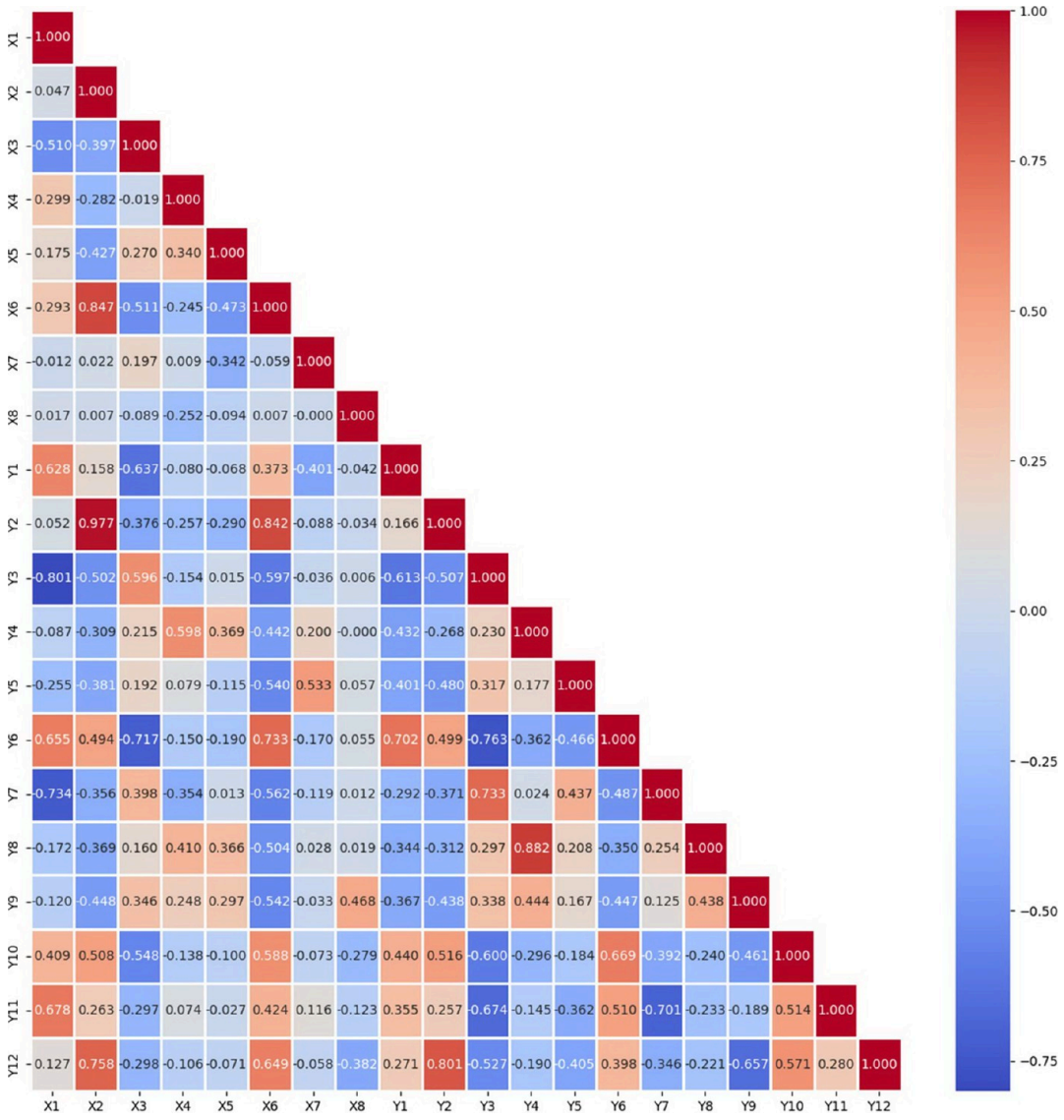

Figure 4. Pearson correlation matrix for the obtained data set.

in some experiments are associated with maximum initial loads (about 6 mg N/L) and insufficient aeration intensity at the second stage. The Pearson correlation matrix (Figure 5) revealed important relationships among the parameters of the initial water, process factors, and the quality of purified water at different stages of the two-stage water treatment system.

The Pearson correlation matrix shows that iron in the initial water (X1) exhibits a pronounced reducing effect of its dissolved forms, mainly Fe^{2+}, as evidenced by a strong negative correlation with the oxidation−reduction potential after both stages (Y3 and Y7) with high coefficients (−0.801 and −0.734). This is explained by the predominance of Fe^{2+} in the initial water, which, during active oxidation to Fe^{3+} at the first stage (primary aeration with subsequent filtration), acts as a reducing agent. Despite the expected increase in the oxidation−reduction potential (Eh) during oxidation, a weakening of the Eh growth after the second stage was experimentally observed, which indicated the presence of other reducing agents (organic compounds or N-NH_4^+). The behavior of ammonium nitrogen, demonstrating fundamentally different patterns at different stages of purification, deserves special attention. The maximum efficiency of its removal is achieved at the second stage, where, in the absence of aeration at the second stage (X8 = 0), the efficiency of purification for ammonium nitrogen is only 39.5%, which convincingly proves the critical importance of aeration at this stage. The strongest positive relationship (0.985) between ammonium nitrogen in the source water (X2) and its content after the first stage (Y2) indicates an extremely low efficiency of ammonium removal at this stage, which is typical for physicochemical methods. The relationship between ammonium nitrogen in the source water (X2) and its content after the second stage (Y12) (strong positive correlation equal to 0.781) indicates a higher efficiency of the second stage. However, complete removal of N-NH_4^+ does not occur and at some parameters even exceeds the standard values. This is due to the resistance of ammonium compounds to oxidation, which indicates the need to optimize the corresponding processes. From this analysis, it follows that the N-NH_4^+ load and the intensity of aeration at the second stage of purification are the determining factors.

The analysis of the oxidation processes also revealed another important relationship. The increase of Eh in the feedwater (X3) leads to the decrease of COD-Mn (Y6) after the first stage (strong negative correlation equal to −0.717). This is

https://doi.org/10.1021/acsestwater.5c01127
ACS EST Water 2026, 6, 1083−1097

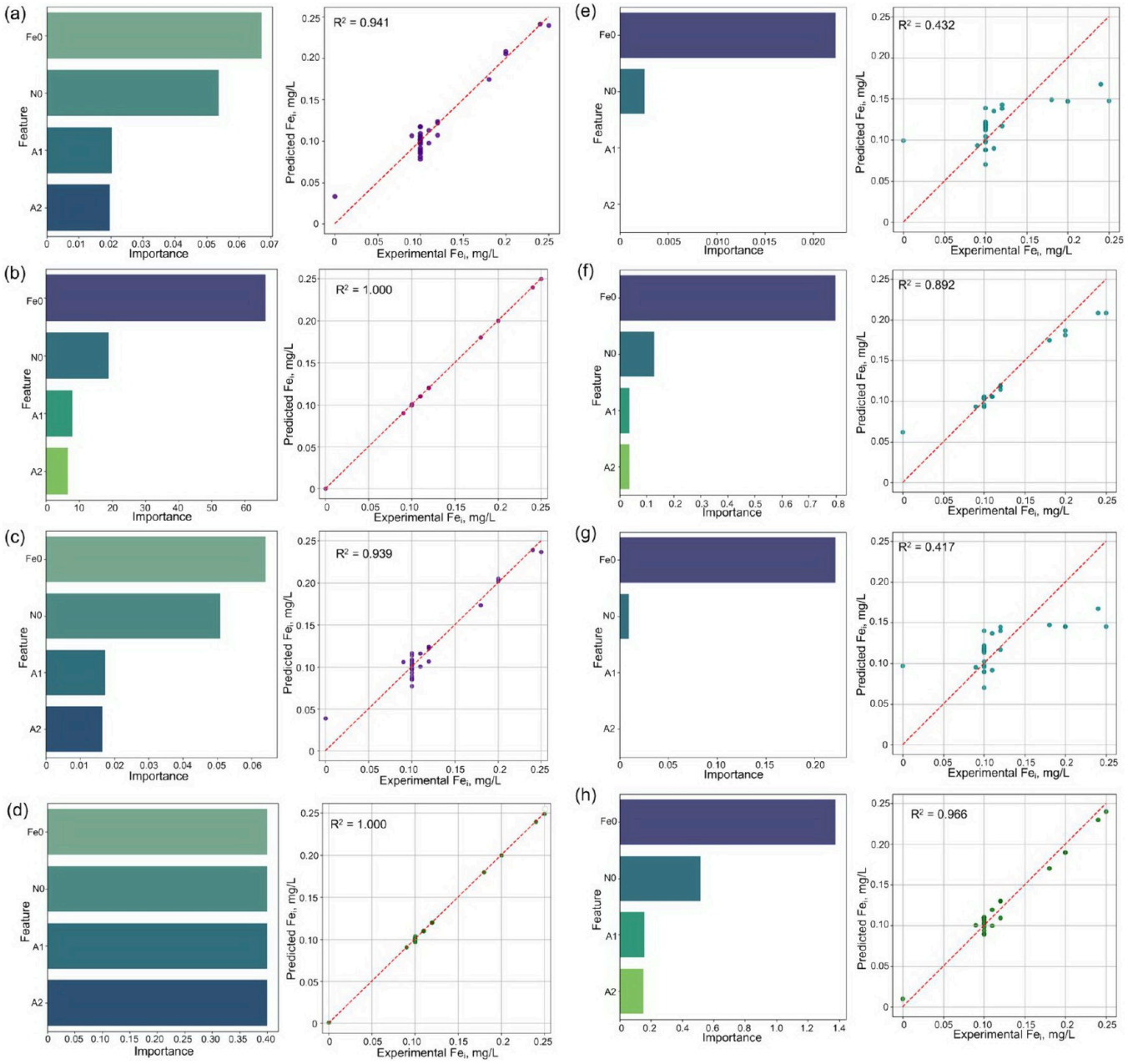

Figure 5. Determination coefficients, variable importance, and plots of predicted and measured values for Fe_i (mg/L) for the polynomial equation (a), CatBoost (b), ElasticNet-poly (c), GPR (d), ElasticNet (e), eXGBoost (f), eLasso (g), and SVR (h).

explained by the fact that a higher Eh contributes to more efficient oxidation of organic substances measured by COD-Mn. This effect is enhanced as the water passes through the purification system, demonstrating a strong negative correlation (strong negative correlation equal to −0.763) between ORP and COD-Mn after the first stage (Y3 and Y6). At the same time, the increase in ORP after the first stage (Y3) leads to the growth of ORP after the second stage (Y7; strong positive correlation equal to 0.733), which indicates the intensification of electrochemical equilibrium processes and the possibility of more complete oxidation of substances. This confirms that ORP is an important parameter controlling the rate and depth of oxidation of an organic substance. A direct relationship between the COD-Mn of the initial water (X6) and the COD-Mn after the first stage (Y6; strong positive correlation equal to 0.733) is also noted. Increased initial organic load leads to higher residual COD-Mn after treatment because the processes of oxidation and sorption of organic matter have their efficiency limits. In addition, the relationship between COD-Mn of the initial water (X6) and ammonium after the first stage (Y2; strong positive correlation equal to 0.842) indicates possible general anthropogenic pollution: situations with a high content of biodegradable organic matter are often accompanied by elevated concentrations of ammonium. A strong positive correlation between ammonium nitrogen (X2) and COD-Mn of the feedwater (X6) (a strong positive correlation of 0.851) is an important feature confirming the hypothesis of an anthropogenic source of pollution (wastewater and agricultural runoff), where elevated concentrations of ammonium nitrogen are often accompanied by a high content of biodegradable organic matter, requiring more intensive purification methods. As for the output data, a

https://doi.org/10.1021/acsestwater.5c01127
ACS EST Water 2026, 6, 1083−1097

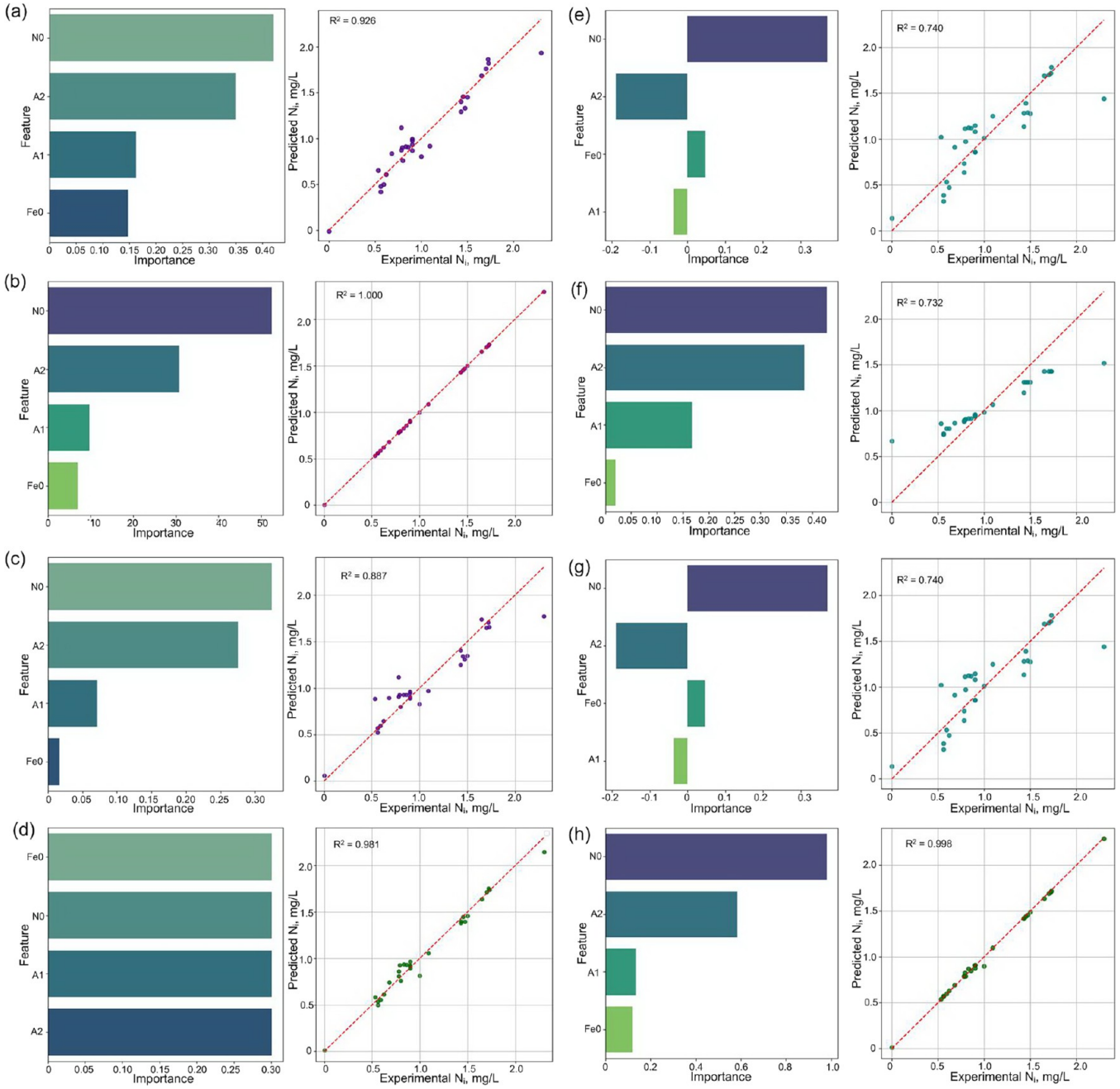

Figure 6. Determination coefficients, variable importance, and plots of predicted and measured values for N_i (mg/L) for polynomial equation (a), CatBoost (b), ElasticNet-poly(c), GPR (d), ElasticNet (e), eXGBoost (f), eLasso (g), and SVR (h).

direct correlation between iron and COD-Mn after the first stage (Y1 and Y6; a strong positive correlation of 0.702) indicates the possibility of forming its organic complexes (humates) at a high iron content, which increases the need for oxidizing agents and complicates their removal. A negative correlation between Eh after the second stage (Y7) and iron after the second stage (Y11; equal to −0.701) confirms the thermodynamic basis for iron purification. High Eh (strictly oxidizing conditions) at the outlet of the second stage is a guaranteed indication of complete oxidation of Fe^{2+} to Fe^{3+} and its subsequent precipitation.

It is worth noting that the change in pH after the first stage has a significant effect on its value after the second stage. The increase in pH at the outlet of the second stage is associated with an increase in pH at the inlet of the first. This is crucial to consider when balancing chemical reagents to prevent equipment corrosion and maintain process stability. Analysis of the effect of aeration before the first stage (X7) shows that it moderately reduces iron (Y1; negative correlation equal to −0.401), which corresponds to its main purpose: the oxidation of Fe^{2+} to Fe^{3+} by atmospheric oxygen, which is then easily precipitated or removed during filtration. Similarly, a decrease in the level of COD-Mn (Y6; negative correlation equal to −0.170) indicates partial oxidation of organic matter under the influence of oxygen, which confirms the importance of aeration for enhancing oxidation processes. It is interesting to note that an increase in the air supply ratio before the first stage contributes to an increase in pH (Y4, insignificant positive

https://doi.org/10.1021/acsestwater.5c01127
ACS EST Water 2026, 6, 1083−1097

correlation equal to 0.200) and an increase in DO (Y5; positive correlation equal to 0.533). This is explained by the fact that water saturation with oxygen promotes neutralization of acidic components and an increase in pH due to the oxidation reaction of organic substances with the formation of hydroxides or other alkaline compounds. An increase in the level of DO creates favorable conditions for further oxidation processes and the stabilization of the chemical composition of water. At the same time, a slight decrease in ammonium nitrogen is observed (Y2, close to zero correlation equal to 0.088), which indicates that primary aeration has minimal influence on ammonium removal since this process mainly depends on stages of subsequent treatment. Similarly, an increase in the air supply ratio before the second stage (X8) leads to a significant increase in DO (Y9; positive correlation equal to 0.468), which significantly enhances possibilities of oxidation of organics and metals. As a result, a decrease in the COD-Mn concentration (Y10; minor negative correlation equal to −0.290) and a decrease in the total iron content (Y1; minor negative correlation equal to −0.123) are observed after the second stage. These data confirm the high efficiency of aeration in removing iron and organic contaminants in the second stage of treatment. Most importantly, this is a noticeable decrease in ammonium nitrogen after the second stage (Y12; positive correlation equal to 0.382), which indicates the removal of ammonium due to secondary aeration. This is because water saturation with oxygen stimulates nitrification processes by microorganisms or chemical reactions of oxidation of ammonium to nitrites and nitrates in the presence of zeolite.

Summarizing the results of the studies, we can conclude that aeration is a key factor in increasing the efficiency of iron and organic matter removal due to the enhancement of oxidation processes when water is saturated with oxygen. At the same time, optimizing the air-to-water ratio before each stage allows one to control the level of DO and the pH of the water: increasing this ratio helps to increase the pH and DO without significantly affecting the ammonium content at the first stage. In turn, monitoring (observation, assessment, and forecast) of Eh and pH at all stages is the most important tool for operational control and management of the purification efficiency.

3.2. Modeling

For operation of the purification system, the primary parameters for the operator are using the initial concentrations of iron and ammonium nitrogen, setting the aeration intensity at each of the stages, and providing the final concentrations of iron and ammonium nitrogen to the established standards. This section provides a comprehensive comparative analysis of various mathematical models used to describe and predict the operation of a two-stage groundwater purification system with a complex composition. The main task of the modeling was to identify the dependence of the residual concentrations of total iron (Y11) and ammonium nitrogen (Y12) at the outlet of the unit on the initial water indicators (X1 and X2) and the aeration regime parameters at the first (X7) and second (X8) filtration stages. To ensure the correctness of the assessment, a wide range of models were used, from classical polynomial regression to machine-learning methods including CatBoost, eXGBoost, GPR, ElasticNet (with and without polynomial features), and eLasso. Each model was tested for the coefficient of determination and analyzed for the physicochemical interpretability of the obtained coefficients.

The basic second-order polynomial model (Figures 5a and 6a) demonstrated an acceptable quality of process description: for iron, R^2 was 0.758, and for ammonium nitrogen, it was 0.967:

$$\begin{aligned} Y11 = {} & 0.098 + 0.030X1 + 0.011X2 + 0.004X7 \\ & - 0.007X8 + 0.013X1^2 + 0.022X1X2 - 0.001X1X7 \\ & + 0.001X1X8 + 0.003X2^2 + 0.009X2X7 - 0.009X2X8 \\ & + 0.004X7^2 + 0.002X7X8 - 0.001X8^2 \end{aligned} \quad (1)$$

$$\begin{aligned} Y12 = {} & 0.836 + 0.046X1 + 0.363X2 - 0.026X7 \\ & - 0.193X8 - 0.029X1^2 + 0.033X1X2 + 0.030X1X7 \\ & + 0.009X1X8 + 0.007X2^2 - 0.014X2X7 + 0.003X2X8 \\ & + 0.091X7^2 + 0.001X7X8 + 0.144X8^2 \end{aligned} \quad (2)$$

The highest R^2 values (1.000 for both variables) were shown by the CatBoost model (Figures 5b and 6b).

The ElasticNet model with polynomial features (ElasticNet-poly, Figures 5c and 6c) showed R^2 values of 0.939 for iron and 0.887 for ammonium. Optimal regularization parameters (alpha and l1_ratio) ensured the elimination of multicollinearity while maintaining physically reasonable coefficients: for Fe, R^2 = 0.939, optimal α = 0.00066, and optimal l1_ratio = 0.9, and for N, R^2 = 0.887, optimal α = 0.03556, and optimal l1_ratio = 1.0.

$$\begin{aligned} Y11 = {} & 0.099 + 0.030X1 + 0.010X2 + 0.004X7 \\ & - 0.006X8 + 0.012X1^2 + 0.022X1X2 + 0.003X2^2 \\ & + 0.008X2X7 - 0.008X2X8 + 0.003X7^2 + 0.002X7X8 \end{aligned} \quad (3)$$

$$\begin{aligned} Y12 = {} & 0.859 + 0.015X1 + 0.325X2 - 0.154X8 \\ & - 0.002X1^2 + 0.071X7^2 + 0.122X8^2 \end{aligned} \quad (4)$$

For iron, the initial concentrations of both Fe_0 and the product $Fe_0{\cdot}N_0$ turned out to be the most important, which reflects the mutual influence of iron and ammonium on the rate of the oxidation processes. For ammonium nitrogen, the quadratic terms for aeration ($A1^2$ and $A2^2$) became significant, confirming the presence of optimal values of the air/water ratio, at which a maximum removal efficiency is achieved. A high level of accuracy for iron was achieved by the GPR model (Figures 5d and 6d) with a radial basis kernel (R^2 = 1.000 for iron and R^2 = 0.981 for ammonium nitrogen). For iron, the trained GPR kernel is 0.1242 RBF (length_scale = 2.5) + WhiteKernel (noise_level = 1×10^{-5}). For ammonium nitrogen, the trained GPR kernel is 1.332 RBF (length_scale = 3.32) + WhiteKernel (noise_level = 0.0136).

The use of "pure" ElasticNet (Figures 5e and 6e) without polynomial features gave lower R^2 (0.432 for iron and 0.740 for ammonium), which indicates the need to consider nonlinear effects in such systems. For iron, the optimal l1_ratio is 0.1, and the optimal α value is 0.09102981779915217. For ammonium nitrogen, the optimal l1_ratio is 1.0, and the optimal α value is 0.0001264855216852957. In this model, as well as for the standard polynomial and ElasticNet-poly for iron, the important parameters are the initial concentrations of iron and ammonium nitrogen, and for ammonium nitrogen, the most significant in the equation are the aeration intensities:

https://doi.org/10.1021/acsestwater.5c01127
ACS EST Water 2026, 6, 1083−1097

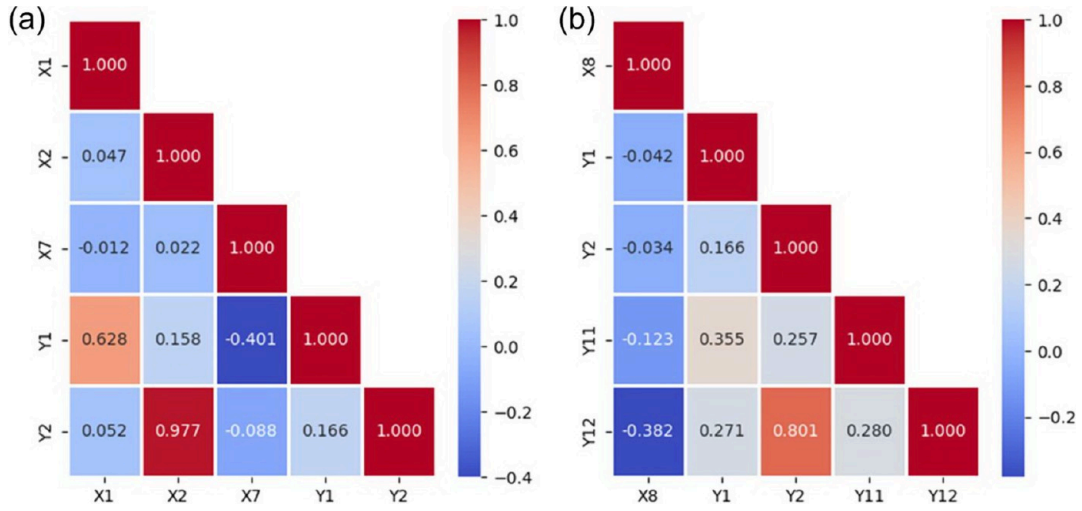

Figure 7. Pearson correlation matrix for the first stage (a) and second stage (b) of purification.

$$Y11 = 0.119 + 0.022X1 + 0.003X2 \quad (5)$$

$$Y12 = 1.050 + 0.047X1 + 0.370X2 - 0.036X7 - 0.190X8 \quad (6)$$

The eXGBoost method (Figures 5f and 6f) demonstrated good results (R^2 = 0.892 for iron and R^2 = 0.732 for ammonium), which is explained by its ability to detect nonlinear threshold dependencies. A similar situation was observed for ElasticNet and eLasso (Figures 5g and 6g), where regularization (the absence of polynomial features) strongly zeroed out weak connections and R^2 for iron was only 0.417. However, for ammonium, eLasso retained good quality (R^2 = 0.740), which is due to a simpler dependence of its residual concentration on the regime parameters:

$$Y11 = 0.119 + 0.022X1 + 0.001X2 \quad (7)$$

$$Y12 = 1.050 + 0.047X1 + 0.370X2 - 0.036X7 - 0.190X8 \quad (8)$$

The SVR (Figures 5h and 6h) model gives high R^2 = 0.966 for Fe (RMSE = 0.009) and R^2 = 0.998 for Fe (RMSE = 0.024).

The analysis of the models showed that, for the tasks of operational control of the technological process, it is advisible to use polynomial regression equations or ElasticNet-poly because they provide a sufficiently high accuracy while maintaining physicochemical interpretability. For forecasting under conditions of sharp fluctuations in water composition and when developing strategies for optimizing aeration modes, GPR and gradient boosting (CatBoost and eXGBoost) are more preferable because they are most sensitive to complex nonlinear interactions of factors. A comparison of the modeling results with full-scale experiments confirmed their practical applicability: the efficiency of ammonium removal is largely determined by the intensity of aeration, and the efficiency of iron removal strongly depends on the initial content of ammonium nitrogen. Thus, the modeling confirmed the key role of air−water ratio control at both stages, while for the first stage (with the AC sorbent), the priority is to achieve the maximum oxidation rate of Fe^{2+}, and for the second stage (zeolite), it is maintaining the sorption capacity of the material.

It should be emphasized that the CatBoost and GPR models in this study were used as interpolating regression tools, not as predictive machine-learning models intended for generalization. The entire experimental data set (n = 29) was used for model fitting without train/test splitting; therefore, flexible algorithms such as CatBoost and GPR with RBF kernels naturally reproduce the data set with negligible residuals, yielding R^2 values close to 1.000. This result reflects a near-exact interpolation of the measurement points rather than an overfitting in the classical machine-learning sense because extrapolative prediction was not the purpose of the modeling framework. For operational use, simpler physically interpretable polynomial and ElasticNet-poly models were selected. It is important to clearly distinguish between the empirical results of the laboratory campaign and the conclusions derived from the regression modeling. The empirical observations refer exclusively to direct measurements obtained from the 29 experimental modes, including the documented influence of the aeration intensity on the Fe^{2+} oxidation rates and the observed inhibitory effect of ammonium nitrogen. In contrast, the modeling results represent computational interpretations generated from the regression tools (Polynomial, ElasticNet-poly, SVR, and GPR), which describe the structure of nonlinear dependencies, quantify factor interactions, and visualize response surfaces. While the empirical data define the actual performance of the treatment system under the tested conditions, the modeling output provides an analytical framework for interpreting these trends and should be understood as an approximation confined to the experimental domain.

3.3. Evaluation of the Influence of Parameters on the Removal of Iron and Ammonium Nitrogen in Two Stages of Purification

This section analyzes the operation of each of the purification stages in the proposed scheme. The Pearson correlation matrix (Figure 7a) for the first stage shows correlations between the iron concentrations in the feedwater (X1) and ammonium nitrogen (X2), the degree of aeration (X7), and the output parameters (Y1 and Y2). The degree of aeration (X7) has the greatest impact on the residual iron concentration (Y1), which is manifested in a negative correlation (−0.401). This is consistent with the fundamental principle that increasing the

https://doi.org/10.1021/acsestwater.5c01127
ACS EST Water 2026, 6, 1083−1097

air supply enhances the transition of Fe^{2+} to Fe^{3+} through the following reaction:

$$4Fe^{2+} + O_2 + 10H_2O \rightarrow 4Fe(OH)_3 \downarrow + 8H^+$$

The polynomial model for Fe_i (Y1; $R^2 = 0.758$) is as follows:

$$\begin{aligned} Y1 = {} & 0.0987 + 0.1107X1 + 0.1989X2 - 0.1256X7 \\ & - 0.0122X1^2 + 0.0021X1X2 + 0.0139X1X7 \\ & - 0.0249X2^2 - 0.0026X2X7 + 0.0055X7^2 \end{aligned} \quad (9)$$

Analysis of the significance of factors (Figure S1) shows the dominant role of the degree of aeration (X7), and its contribution to the model is almost 4.2 times greater than the influence of X2. The polynomial model for Ni (Y2; $R^2 = 0.967$) is as follows:

$$Y2 = 0.4173 + 0.0042X1 + 0.8359X2 - 0.1181X7 \quad (10)$$

The factor importance plot (Figure S2) for the ammonium removal efficiency after the first stage (Y2) also shows the dominance of the aeration rate (X7) with an importance value of ~1.7 conventional units, while the concentrations of iron (X1) and ammonium (X2) in the feedwater show an importance close to 0 conventional units. Thus, the matrix data showed that X7 has a unique dual mechanism of action: (i) intensification of Fe^{2+} oxidation to Fe^{3+} for iron; (ii) CO_2 desorption, a shift of the $NH_4^+ \leftrightarrow NH_3 + H^+$ equilibrium, and NH_3 volatilization (the target degassing mechanism) for ammonium nitrogen.

The correlation analysis of the second treatment stage also revealed complex relationships between the process parameters (Figure 7b). For ammonium nitrogen (Y12), the most pronounced dependence on its content after the first stage (Y2) is observed with a correlation coefficient of 0.801, which confirms the predominance of physicochemical removal mechanisms at this stage. A polynomial model for residual iron (Y11) with a high determination coefficient ($R^2 = 0.9539$; Figure S3):

$$\begin{aligned} Y11 = {} & 0.1752 - 2.3603X8 + 2.2301Y1 + 0.3080Y2 \\ & + 1.3448X8^2 + 3.4829X8Y1 + 0.0421X8Y2 \\ & - 1.1519Y1^2 - 2.2986Y1Y2 + 0.0712Y2^2 - 0.0815X8^3 \\ & - 1.8139X8^2Y1 - 0.0285X8^2Y2 + 0.2271X8Y1^2 \\ & - 0.0216X8Y1Y2 + 0.0008X8Y2^2 + 0.1524Y1^3 \\ & + 0.2313Y1^2Y2 + 0.3517Y1Y2^2 - 0.0232Y2^3 \end{aligned} \quad (11)$$

The analysis of the significance of factors (Figure S3) shows the dominant role of the iron content after the first stage (Y1 ~ 900 conventional units). The weak influence of ammonium after the first stage (Y2 ~ 150 conventional units) and the lack of significance of aeration (X8 ~ 0 conventional units) show that the efficiency of iron removal at the second stage is determined mainly by its concentration at the inlet (Y1) and not by the efficiency of aeration at the second stage. That is, aeration at the second stage is almost entirely focused on the oxidation of ammonium nitrogen ($R^2 = 0.9209$):

$$\begin{aligned} Y12 = {} & 0.6822 - 1.4008X8 + 1.0684Y1 + 0.1910Y2 \\ & + 0.6763X8^2 - 0.9152X8Y1 + 0.0223X8Y2 \\ & + 0.6472Y1^2 - 0.1057Y1Y2 + 0.0153Y2^2 \end{aligned} \quad (12)$$

The analysis of the equation revealed a strong contribution of the aeration intensity: 1.4008X8 and 0.6763$X8^2$ (Figure S4).

The general correlation matrix for the selected parameters for modeling (using initial concentrations of iron and ammonium nitrogen, setting the aeration intensity at each of the stages, and providing the final concentrations of iron and ammonium nitrogen to the established standards) with the addition of such factors as the overall efficiency of iron removal (Y13, %), the rate constant of the iron oxidation reaction (Y14, s^{-1}), the overall efficiency of N-NH_4^+ removal (Y15, %), and the rate constant of the N-NH_4^+ oxidation reaction (Y16, s^{-1}) is presented in Figure 8. An analysis of the correlation matrix

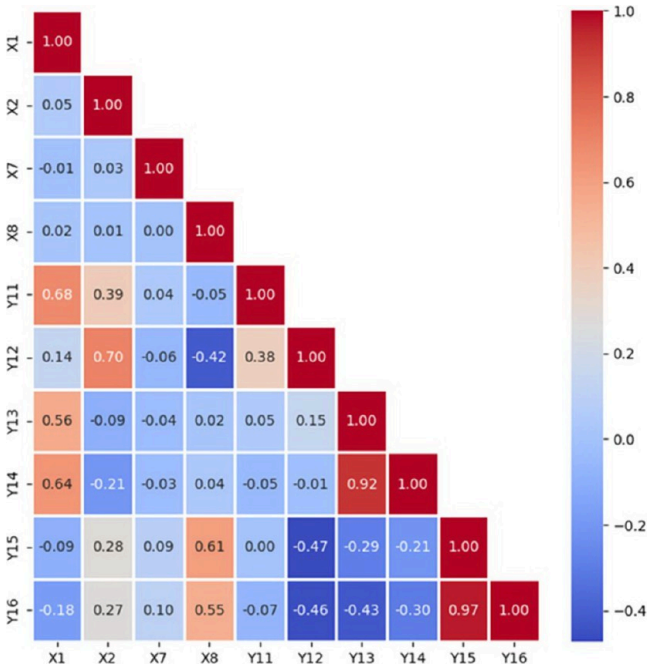

Figure 8. General correlation matrix with the addition of efficiency indicators (Fe and N-NH_4^+ oxidation efficiency and Fe and N-NH_4^+ oxidation reaction rate constants).

(Figure 8) revealed a strong correlation between the purification efficiency and process rates: for iron ($r = +0.92$ between Y13 and Y14) and for ammonium ($r = +0.97$ between Y15 and Y16), confirming the crucial role of oxidation and sorption kinetics in the overall efficiency of the technology. Thus, the analysis confirmed the cascade principle of the system: the first stage is responsible for the oxidation and removal of the bulk of the iron and the second for ammonium sorption, the efficiency of which is limited by residual iron. A practical consequence is the need to maintain the iron concentration after the first stage at a level of ≤0.3 mg/L to ensure stable operation of the zeolite bed in the second stage.

Although the observed decrease in the ammonium removal efficiency at elevated residual iron concentrations is consistent with several known physicochemical pathways, the underlying mechanism cannot be fully resolved based on the current experimental data set. Possible contributing factors include (i) competition between Fe^{2+} oxidation and nitrification for DO; (ii) modification of the biofilm activity due to the accumulation of freshly precipitated iron(III) hydroxides; (iii) catalytic or inhibitory effects related to surface-bound iron species. The available evidence indicates that these processes may act simultaneously; however, the relative contribution of each remains uncertain. Therefore, the interaction between residual iron and ammonium removal

https://doi.org/10.1021/acsestwater.5c01127
ACS EST Water 2026, 6, 1083−1097

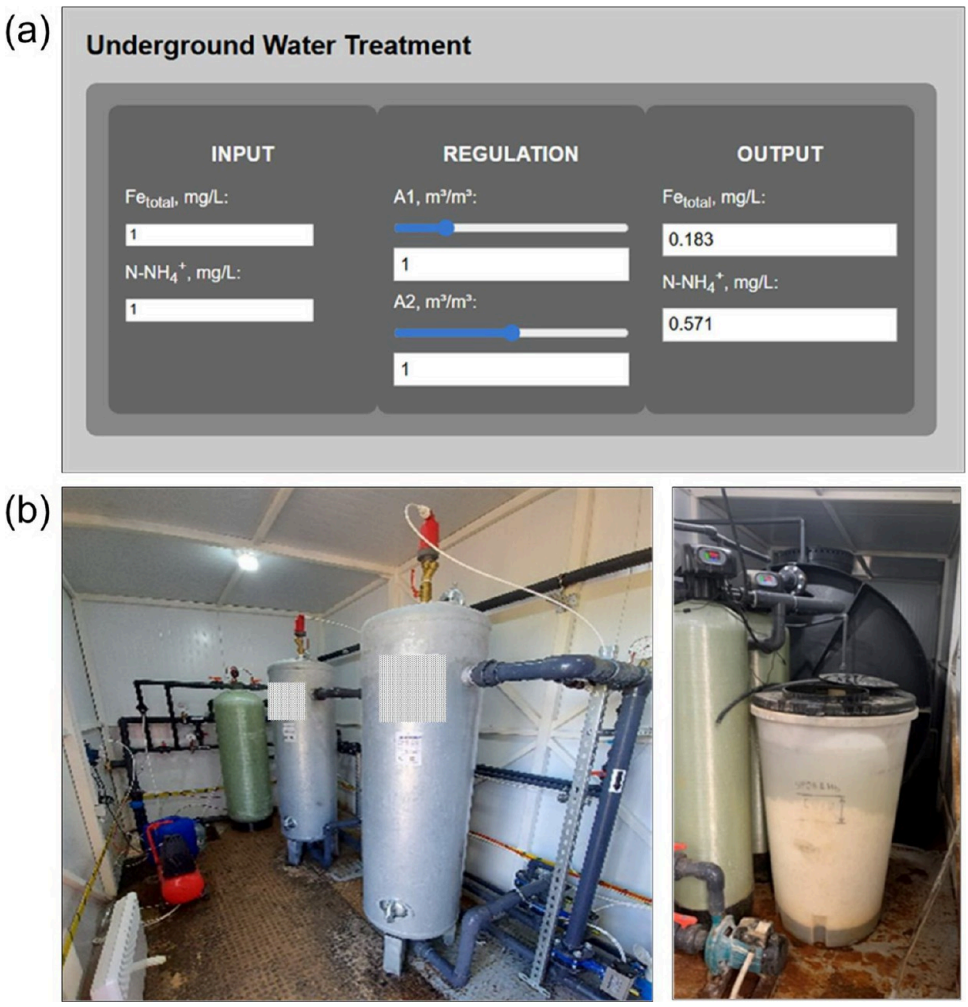

Figure 9. Example of an online platform for the prompt selection of the optimal aeration intensity at each stage of purification (a). Modernized water treatment plant with second stage purification (b) where the first stage (iron removal) consists of an aeration column and two industrial steel filters with a granular AC sorbent bed (left) and the second stage (ammonium removal) consists of two filters with a zeolite bed and a regeneration tank with an 8% NaCl solution (right). The second stage of aeration column is not shown in the photograph.

remains only partially understood in this study. Future work should incorporate targeted kinetic experiments and microbial analyses to identify the dominant pathway. A moderate positive correlation was found between residual iron after the second stage (Y11) and residual ammonium nitrogen after the second stage (Y12; r = 0.381 and p = 0.041; Figure S7), indicating a statistically significant trend: as Y11 increases, Y12 increases; i.e., a higher amount of residual Fe is associated with worse N-NH_4^+ removal ($\alpha \approx 0.05$). Moreover, the correlation between Y11 and the ammonium concentration after the first stage (Y2) was slightly higher (R = 0.418 and p = 0.024; Figure S7), while the relationship between iron after the first stage (Y1) and Y12 was weaker and statistically insignificant (r = 0.271 and p = 0.156). Thus, the data indicate that it is the residual iron remaining in the system after treatment that is associated with elevated ammonium levels in the effluent, suggesting that residual Fe rather hinders (or at least correlates with impairment of) N-NH_4^+ removal. A literature review allows us to identify several plausible mechanisms explaining the effect of residual iron on ammonium removal and compare them with the data obtained. First, competition for DO[31] between Fe^{2+} oxidation and nitrification may reduce O_2 availability for AOB/NOB, which is consistent with the positive Y11−Y12 correlation ($r \approx 0.38$). Second, precipitation of iron(III) hydroxides on the bed surface may physically block sorption sites and biofilms, which is particularly plausible for the second stage, where the correlation with Y11 is most pronounced.[32,33] Third, the alternative pathway of nitrogen removal via Feammox in an aerated system is not supported. An increase in residual Fe is accompanied by an increase in N-NH_4^+ and not a decrease.[34] Fourth, the accumulation of Fe^{3+} and iron flocs can modify the microbial community and suppress the activity of ammonium-oxidizing bacteria, which is also consistent with the observed relationship. Finally, changes in pH and Eh caused by iron and organic matter oxidation processes can affect the NH_4^+/NH_3 equilibrium and inhibit nitrification, which is supported by the identified relationships between Fe, COD, and environmental parameters.[35] Thus, the totality of the data indicates that it is residual iron after the second stage that plays a key role in the deterioration of ammonium removal, acting through several interrelated mechanisms. Based on the literature review and the obtained correlations, the most plausible explanatory hypothesis is a combination of two factors. First, the physicochemical effect associated with the accumulation of iron(III) hydroxides on the surface of the bed (especially in the second stage with

https://doi.org/10.1021/acsestwater.5c01127
ACS EST Water 2026, 6, 1083−1097

zeolite) leads to a decrease in the sorption capacity and site availability for N-NH_4^+ or to pore blockage, which is confirmed by the data.[36,37] Second, competition for oxygen and microbial suppression: ongoing oxidation of Fe^{2+} consumes dissolved O_2 and forms Fe(III) flocs that cover and suppress the nitrifying biofilm, reducing AOB/NOB activity and the efficiency of biological nitrification, which is consistent with studies on the competition for DO and the effect of Fe^{3+}on microbial communities. In the obtained data, this is manifested as follows: residual iron after the second stage (Y11) serves as an indicator of either insufficient/suboptimal aeration or the accumulation of iron deposits on the bed, and it is with an increase in Y11 that a deterioration in ammonium removal is observed.

3.4. Practical Application

In real conditions, knowing the change in the incoming concentrations of iron and ammonium nitrogen, it is necessary to select the values of aeration efficiency at each stage to achieve the required cleaning effect at the outlet of the plant for total iron and ammonium nitrogen. To do this, the dependencies for iron Y11 = f(X1,X2,X7,X8) and ammonium nitrogen Y12 = f(X1,X2,X7,X8) were found.

$$\begin{aligned} Y11 = {} & 0.2859 - 0.0639X1 - 0.0416X2 - 0.0325X7 \\ & + 0.0207X8 + 0.0067X1^2 + 0.0104X1X2 - 0.0007X1X \\ & 7 + 0.0013X1X8 + 0.0012X2^2 + 0.0044X2X7 \\ & - 0.0126X2X8 + 0.0025X7^2 + 0.0040X7X8 \\ & - 0.0028X8^2 \quad (R^2 = 0.9407) \end{aligned} \tag{13}$$

The obtained model (R^2 = 0.9407; Figure S5) shows the dominant influence of the initial ammonium concentration (X2) and the aeration intensity at the first (X7) and second stages (X8) on iron oxidation. The factors' significance (Figure S5) quantitatively confirms this order: X2 (6 conventional units) > X7 (3 conventional units) > X8 (1.5 conventional units).

$$\begin{aligned} Y12 = {} & 1.9488 + 0.0071X1 + 0.1762X2 - 0.4579X7 \\ & - 1.8941X8 - 0.0154X1^2 + 0.0153X1X2 \\ & + 0.0177X1X7 + 0.0146X1X8 + 0.0029X2^2 \\ & - 0.0074X2X7 + 0.0042X2X8 + 0.0591X7^2 \\ & + 0.0020X7X8 + 0.6982X8^2 \end{aligned} \tag{14}$$

The obtained model for groundwater purification from ammonium nitrogen (R^2 = 0.9258; Figure S6) shows the key role of aeration at the second stage (X8) and the contribution of aeration at the first stage (X7) (Figure S6).

These models show good reproducibility and allow real-time calculation of the optimal aeration intensity at each of the purification stages (X7 and X8) with changes in the initial concentrations of iron and ammonium nitrogen at the inlet to the system (X1 and X2), ensuring residual concentrations within the MPC (Fe, ≤0.3 mg/L; N-NH_4^+, ≤1.5 mg/L). These models can be integrated into the online monitoring and automated control system of the plant (SCADA), ensuring stable purification quality with variations in the initial water composition. This will provide adaptive regulation of purification modes in real time. As an example of such software, the following online platform can be proposed (Figure 9a and SI-file.html).

The practical implementation of the proposed second stage of purification allowed one to achieve a reduction in residual iron by 35−45% in practice compared to a single-stage scheme, a reduction in energy costs by 15−20% due to precise dosing of aeration, and stable purification quality with fluctuations in the composition of the incoming water. After the studies, the pilot plant was replaced with industrial filters of the second stage (Figure 9b). The purification results fully corresponded to the indicators obtained at the pilot plant. This technological scheme has been operating for 3 years and shows positive results for ammonium nitrogen, COD-Mn, and iron.

4. CONCLUSIONS

The experiments showed that when using the proposed two-stage scheme with aeration, the iron concentration was stably reduced to the standard 0.3 mg/L, and the residual ammonium content in optimal modes was reduced to a level below 1.5 mg/L with the initial maxima of 6.9 mg/L total iron and 6.0 mg/L ammonium nitrogen. It was shown that the lack of aeration at the second stage reduced the ammonium removal efficiency to 39.5%, while with optimal parameters, the purification efficiency reached 75−80%. The best results were shown by the machine-learning methods CatBoost and GPR (R^2 = 1.000 and 0.981, respectively), as well as ElasticNet with polynomial features (R^2 = 0.939 for Fe and R^2 = 0.887 for N-NH_4^+). The second-order polynomial regression equations also demonstrated an acceptable quality (R^2 = 0.758 for iron and R^2 = 0.967 for ammonium), which confirms the need to consider nonlinear effects. At the same time, simple linear models (ElasticNet without polynomial features and eLasso) gave significantly worse results (R^2 < 0.5 for iron), which shows their limited applicability for describing complex oxidation and sorption processes.

Analysis of the Pearson correlation matrix and the constructed models showed that, for iron, its initial concentration and interaction with ammonium nitrogen at the first stage of purification play a critical role. For ammonium nitrogen, the decisive factor was the intensity of aeration at the second stage. This parameter determines the achievement of the standard values. It was also shown that aeration at the first stage has a moderate effect on the oxidation of iron and organic matter but has virtually no effect on the removal of ammonium. The use of machine-learning equations and algorithms made it possible to construct the dependencies Y11 = f(X1,X2,X7,X8) for iron and Y12 = f(X1,X2,X7,X8) for ammonium with determination coefficients of up to 0.94−0.93. These dependencies make it possible to determine the optimal aeration values at each stage in real time depending on the current composition of groundwater. Practical implementation of the proposed technology at an existing water treatment plant showed that the introduction of the second purification stage ensures a 35−45% reduction in residual iron compared to a single-stage scheme, a 15−20% reduction in energy costs due to precise regulation of aeration, and stable purification quality with fluctuations in the initial concentrations of pollutants. Thus, the integration of two-stage aeration with machine-learning methods ensures reliable achievement of standards for Fe and N-NH_4^+ and is a promising direction for the modernization of iron removal stations in small settlements.

https://doi.org/10.1021/acsestwater.5c01127
ACS EST Water 2026, 6, 1083−1097

■ ASSOCIATED CONTENT

Data Availability Statement

The data that support the findings of this study are available from the corresponding author upon reasonable request.

Supporting Information

The Supporting Information is available free of charge at https://pubs.acs.org/doi/10.1021/acsestwater.5c01127.

Original data set (XLSX)

HTML program implementing the optimal model and allowing for reproducing the calculations (ZIP)

Document with feature importance plots (for eqs 9−14) and a comparison table of model accuracies (R^2, RMSE, and MAE) (PDF)

■ AUTHOR INFORMATION

Corresponding Author

Valentin Romanovski − *Department of Materials Science and Engineering, University of Virginia, Charlottesville, Virginia 22904, United States;* orcid.org/0000-0003-1741-0316; Email: rvd9ar@virginia.edu

Authors

Elena Velyugo − *Department of Department of Heat, Water and Gas Supply, and Ventilation, Polotsk State University, Novopolotsk 211440, Belarus*

Viktor Yushchenko − *Department of Department of Heat, Water and Gas Supply, and Ventilation, Polotsk State University, Novopolotsk 211440, Belarus*

Complete contact information is available at: https://pubs.acs.org/10.1021/acsestwater.5c01127

Author Contributions

V.R.: supervision, conceptualization, methodology, investigation, data curation, formal analysis, validation, software, visualization, writing—original draft, and writing—review and editing. E.V.: investigation, data curation, formal analysis, and writing—original draft. V.Y.: supervision, conceptualization, data curation, formal analysis, and validation. CRediT: **Valentin Romanovski** conceptualization, data curation, formal analysis, investigation, methodology, software, supervision, validation, visualization, writing - original draft, writing - review & editing; **Elena Velyugo** data curation, formal analysis, investigation, writing - original draft; **Viktor Yushchenko** conceptualization, data curation, formal analysis, supervision, validation.

Notes

The authors declare no competing financial interest.

■ REFERENCES

(1) Li, Y.; Ge, X.; Du, Y.; Ding, H.; Ji, X.; Zhou, C.; Chen, Y.; Cui, D.; Lu, A. Spatial distribution and genesis of iron, manganese, arsenic, and nitrogen in groundwater of typical areas. *Sci. China Earth Sci.* **2025**, *68*, 2797−2813.

(2) Madhav, S.; Ahamad, A.; Singh, A. K.; Kushawaha, J.; Chauhan, J. S.; Sharma, S.; Singh, P. Water pollutants: sources and impact on the environment and human health. *Sensors in water pollutants monitoring: Role of material* **2020**, 43−62.

(3) Ojha, A.; Tiwary, D. Organic pollutants in water and its health risk assessment through consumption. In *Contamination of Water*; Academic Press, 2021; pp 237−250.

(4) Prapolski, D.; Romanovski, V. Resent advances in underground water deironing and demanganization: Comprehensive review. *Journal of Water Process Engineering* **2025**, *70*, No. 107089.

(5) Propolsky, D.; Romanovski, V. Iron and Manganese Removal from Underground Water: Comprehensive Review of Filter Media Performance and Pathways to Polyfunctional Applications. *Environ. Sci.: Water Res. Technol.* **2025**, *11*, 2499.

(6) Nyer, E. K. *Groundwater Treatment Technology*; John Wiley & Sons, 1992.

(7) Thomas, B.; Vinka, C.; Pawan, L.; David, S. Sustainable groundwater treatment technologies for underserved rural communities in emerging economies. *Sci. Total Environ.* **2022**, *813*, No. 152633.

(8) Romanovski, V.; Romanovskaia, E.; Moskovskikh, D.; Kuskov, K.; Likhavitski, V.; Arslan, M. F.; Beloshapkin, S.; Matsukevich, I.; Khort, A. Recycling of iron-rich sediment for surface modification of filters for underground water deironing. *J. Environ. Chem. Eng.* **2021**, *9* (4), No. 105712.

(9) Romanovski, V. New approach for inert filtering media modification by using precipitates of deironing filters for underground water treatment. *Environmental Science and Pollution Research* **2020**, *27* (25), 31706−31714.

(10) Propolsky, D.; Romanovskaia, E.; Kwapinski, W.; Romanovski, V. Modified activated carbon for deironing of underground water. *Environmental Research* **2020**, *182*, No. 108996.

(11) Kvartenko, O.; Sabliy, L.; Kovalchuk, N.; Lysytsya, A. The use of the biological method for treating iron containing underground waters. *Journal of Water and Land Development* **2018**, *39* (39), 77−82.

(12) Sharma, S. K.; Petrusevski, B.; Schippers, J. C. Biological iron removal from groundwater: a review. *J. Water Supply: Res. Technol. Aqua* **2005**, *54* (4), 239−247.

(13) Hurynovich, A.; Ramanouski, V.. Artifisial replenishment of the deep aquifers. *E3S Web of Conferences*; EDP Sciences, 2018; Vol. *45*, p 00025.

(14) Schoeman, J. J. Evaluation of a South African clinoptilolite for ammonia-nitrogen removal from an underground mine water. *Water SA* **1986**, *12* (2), 73−82.

(15) Le Leuch, L. M.; Bandosz, T. J. The role of water and surface acidity on the reactive adsorption of ammonia on modified activated carbons. *Carbon* **2007**, *45* (3), 568−578.

(16) Ribári, L.; Kollár, G. Removal of ammonia with biological process in the treatment of drinking water. *Period. Polytech. Civil Eng.* **1991**, *35* (1−2), 27−35.

(17) Ye, X.; Nan, J.; Ge, Z.; Xiao, Q.; Liu, B.; Men, Y.; Liu, J. Simultaneous removal of iron, manganese, and ammonia enhanced by preloaded MnO2 on low-pressure ultrafiltration membrane. *J. Membr. Sci.* **2022**, *656*, No. 120641.

(18) Du, X.; Liu, G.; Qu, F.; Li, K.; Shao, S.; Li, G.; Liang, H. Removal of iron, manganese and ammonia from groundwater using a PAC-MBR system: the anti-pollution ability, microbial population and membrane fouling. *Desalination* **2017**, *403*, 97−106.

(19) Nie, J.; Huang, H.; Rao, P.; Chen, H.; Du, X.; Wang, Z.; Zhang, W.; Liang, H. Composite functional particle enhanced gravity driven ceramic membrane bioreactor for simultaneous removal of nitrogen and phosphorus from groundwater. *Chem. Eng. J.* **2023**, *452*, No. 139134.

(20) Chan, M. K.; Abdullah, N.; Rageh, E. H. A.; Kumaran, P.; Tee, Y. S. Oxidation of ammonia using immobilised FeCu for water treatment. *Sep. Purif. Technol.* **2021**, *254*, No. 117612.

(21) El Shafey, A. M.; Abdel-Latif, M.K.; El-Salam, H.M. A. The facile synthesis of poly (acrylate/acrylamide) titanium dioxide nanocomposite for groundwater ammonia removal. *Desalination Water Treatment* **2021**, *212*, 61−70.

(22) Machekhina, K. I. Kinetics of iron ions oxidation by oxygen in water containing ammonium ions, hardness salts and organic substances. *Bashkir Chem. J.* **2022**, *29* (4), 83−90.

(23) Yushchenko, V.; Velyugo, E.; Romanovski, V. Influence of ammonium nitrogen on the treatment efficiency of underground

water at iron removal stations. *Groundwater for Sustainable Development* **2023**, *22*, 100943.
(24) Yushchenko, V.; Velyugo, E.; Romanovski, V. Development of a new design of deironing granulated filter for joint removal of iron and ammonium nitrogen from underground water. *Environ. Technol.* **2024**, *45*, 2735.
(25) Khmel, E.; Hurynovich, A.; Holubava, V.; Romanovski, V. Organizational Models for Managing the Operation of Water Supply Facilities of the Agro-Industrial Complex. *World Water Policy* **2025**, *11* (3), 735−750.
(26) AC Sorbent. https://alsis-ur.ru/sorbent-as/ (accessed 2025-05-25).
(27) Natural Zeolite. https://gidrositi.ru/catalog/napolniteli/tseolit/ (accessed 2025-05-25).
(28) Zeol. https://zeol.ru/ (accessed 2025-05-25).
(29) On the approval of hygiene standards. https://pravo.by/document/?guid=12551&p0=C22100037 (accessed 2025-05-25).
(30) World Health Organization (WHO). Guidelines for Drinking-water Quality: Fourth Edition Incorporating the First and Second Addenda. WHO: Geneva, Switzerland, 2022. https://www.who.int/publications/i/item/9789240045064 (accessed 2025-05-25).
(31) Cheng, Q. Competitive mechanism of ammonia, iron and manganese for dissolved oxygen using pilot-scale biofilter at different dissolved oxygen concentrations. *Water Science and Technology: Water Supply* **2016**, *16* (3), 766−774.
(32) Corbera-Rubio, F.; Kruisdijk, E.; Malheiro, S.; Leblond, M.; Verschoor, L.; van Loosdrecht, M. C.M.; Laureni, M.; van Halem, D. A difficult coexistence: resolving the iron-induced nitrification delay in groundwater filters. *Water Res.* **2024**, *260*, No. 121923.
(33) Wu, T.; Zhong, L.; Pang, J. W.; Ren, N. Q.; Ding, J.; Yang, S. S. Effect of Fe3+ on the nutrient removal performance and microbial community in a biofilm system. *Front. Microbiol.* **2023**, *14*, No. 1140404.
(34) Rodríguez, C.; Cisternas, J.; Serrano, J.; Leiva, E. Nitrogen removal by an anaerobic iron-dependent ammonium oxidation (Feammox) enrichment: potential for wastewater treatment. *Water* **2021**, *13* (23), 3462.
(35) Lytle, D. A.; Williams, D.; Muhlen, C.; Riddick, E.; Pham, M. The removal of ammonia, arsenic, iron and manganese by biological treatment from a small Iowa drinking water system. *Environmental science: water research & technology* **2020**, *6* (11), 3142−3156.
(36) Liu, T.; Wang, H.; Zhang, Z.; Zhao, D. Application of synthetic iron-oxide coated zeolite for the pollution control of river sediments. *Chemosphere* **2017**, *180*, 160−168.
(37) Corbera-Rubio, F.; Kruisdijk, E.; Malheiro, S.; Leblond, M.; Verschoor, L.; van Loosdrecht, M. C.M.; Laureni, M.; van Halem, D. A difficult coexistence: resolving the iron-induced nitrification delay in groundwater filters. *Water Res.* **2024**, *260*, No. 121923.

https://doi.org/10.1021/acsestwater.5c01127
ACS EST Water 2026, 6, 1083−1097